Structural Engineering and Mechanics, *Vol. 74, No. 2 (2020) 215-225*
DOI: https://doi.org/10.12989/sem.2020.74.2.215

Wrinkling of a homogeneous thin solid film deposited on a functionally graded substrate

Masoud Noroozi*

Faculty of Mechatronics, Islamic Azad University (Karaj Branch), Karaj, Iran

(Received June 13, 2019, Revised July 17, 2019, Accepted November 25, 2019)

Abstract. Thin films easily wrinkle under compressive loading due to their small bending stiffness resulting from their tiny thickness. For a thin film deposited on a functionally graded substrate with non–uniform stiffness exponentially changes along the length span in this paper, the uniaxial wrinkling problem is solved analytically in terms of hyper–Bessel functions. For infinite, semi–infinite and finite length systems the wrinkling load and wrinkling wavenumber are determined and compared with those in literature. In comparison with a homogeneous substrate–bounded film in which the wrinkling pattern is uniform along the length span, for a functionally graded substrate–film system the wrinkles accumulate around the softer location of the functionally graded substrate. Therefore, the effective length of the film influenced by the wrinkles decreases, the amplitude of the wrinkles on softer regions of the functionally graded substrate grows and the wrinkling load of the functionally graded substrates with higher softening rate decreases more. The results of the current research are expected to be useful in science and technology of thin films and wrinkling of the structures especially living tissues.

Keywords: thin film; substrate; wrinkling; functionally graded materials; hypergeometric function

1. Introduction

Thin films have many applications in new technologies like energetic films (Clark *et al*. 2015), drug delivery (Karki *et al*. 2016), ion batteries (Jia and Li 2016), solar cells (Zhang *et al*. 2018, Aberle 2009), high temperature thin film devices (Veronese *et al*. 2015) and gel structures (Hu *et al*. 2014). In nature, living tissues including skins, brain, lungs and pulmonary airway can be modeled as a soft substrate covered by a stiff thin surface layer (Amar and Bordner 2017, Li *et al*. 2011, Cerda 2005). Mimicking the pattern formation of fruits during their growing process and leaves during drying process is considered in thin film literature (Chen *et al*. 2014). However, the wrinkling (local instability) of the film may have both negative and positive effects on the functionality of the system (Genzer and Groenewold 2006). As an example of the destructive influence of the wrinkles, Karki and his coworkers (2016) considered drug delivery using thin films where the homogeneity and smoothness of the film is too important. The wrinkles prevent the uniform distribution of drug throughout the polymeric mixture. To avoid wrinkling of the film, they used a liquid wetting agent to ensure that the surface of the substrate is not wrinkled. Jia and Li (2016) investigated the evolution of the wrinkling morphology of a substrate–thin film anode and its effect on the failure of the anode under cyclic charging/discharging. As another example of the destructive effect of the wrinkles, one may refer to the wrinkling of solar sails and membrane antenna in spacecrafts and aerospace structures (Xu *et al*. 2015a). Vonach and Rammerstorfer (2001) studied the sudden failure of the light weight structures made of heterogeneous sandwich plates under wrinkling. Also one may refer to delamination of thin polymer films from compliant substrates due to wrinkling process as noted by Nolte *et al*. (2017).

Besides the destructive effects, wrinkles may have positive influences on the applicability and functionality of the system. For example, Zhang and his coworkers (2018) introduced a silicon–wafer solar cell with wrinkled coating in which the efficiency of the system is increased compared with the unwrinkled surface. In design process of roof and wall cladding in buildings using sandwich panels, Mahendran and Jeevaharan (1999) improved the sustainability of the structure against overall buckling by using wrinkled thin plate–polystyrene core framework. As the result, researchers focused on the developing novel approaches to generate surface wrinkles via different methods to obtain various wrinkling morphologies including wavy shaped, ring–like, checkerboard, stripe, herringbone and hybrid patterns (Fu *et al*. 2018, Song 2010, Chen and Hutchinson 2004).

Wrinkles develop on the film due to its tiny thickness under the context of mechanical instability (i.e. local buckling). Because the bending rigidity of the slender film is very small, it is easily bent under compressive stresses. Different parameters get involved in the wrinkling evolution on the film such as the distribution of the loading (Wang *et al*. 2016, Kudrolli and Chopin 2018, Cerda *et al*. 2002), the boundary conditions of the system, the material properties of the film–substrate (Noroozi and Jiang 2012) and the geometrical uniformity or the inhomogeneity of the system.

The spatial variation in the microstructure or

*Corresponding author, Assistant Professor
E-mail: masoud.noroozi@kiau.ac.ir

http://www.techno-press.com/journals/sem&subpage=7
ISSN: 1225-4568 (Print), 1598-6217 (Online)

composition of the film/substrate, for example in the deposition process of the film on the substrate, may alter the mechanical properties of the system along the thickness direction represented by functionally graded (FG) models. Many practical systems in industry and technology have used functionally graded foundations; and the materials are modeled through the variations of Young's modulus of the foundation along the thickness direction as softening–stiffening behavior of the FG–substrate (Xu *et al*. 2015b, Cao *et al*. 2012, Howarter and Stafford 2010, Lee *et al*. 2008). Cao *et al*. (2012) considered the wrinkling of a hard layer resting on an elastic graded soft substrate subjected to an in–plane compression; while the Young's modulus of the elastic substrate is assumed to vary along its depth direction by power and exponential functions. The critical compressive load at the onset of wrinkling and the wrinkling wavelength are derived analytically and verified by using finite element simulation. A similar research was carried out by Chen *et al*. (2017) in which the wrinkling of the stiff thin film on the semi–infinite elastic graded compliant substrate with variable stiffness along its depth was considered under in–plane compression. The wrinkles were sought analytically in a sinusoidal form for the case with the substrate modulus exponentially decaying along the depth and the critical load and wavelength of the wrinkling were studied. In 2017, Zheng *et al*. investigated the wrinkling of a stiff film resting on a fiber–filled soft substrate, in which the substrate properties changes along the film span and the effects of the cross section dimension, spacing, and positions of the fibers on the wrinkling pattern were investigated. They showed that under compressive loading, different patterns may occur on the film due to the inhomogeneity of the substrate. Yu *et al*. (2016) also considered an elasticity gradient PDMS substrates with nonuniform longitudinal stiffness along the film span experimentally. However, despite its importance, the variation of the substrate properties along the length span of the film is less paid attention by the researchers.

For the film substrate–system, different mechanical models have been presented to consider the mechanical instability of the system. The film is usually modeled by using a membrane, strip or plate with small thickness under compressive loading (Chen and Hutchinson 2004). The film–substrate interaction is modeled with normal and shear reactions on the film. Different models such as Filonenko–Borodich, Pasternak, Hetenyi and Vlasov describing two–parameter foundations have been used to represent the interaction of the beam/film and its foundation reviewed by Wang *et al*. (2005). Amongst different models, Winkler foundation is a common type in which by using a spring system, the interaction of the substrate and the film is corresponding with the deflection of the film and stiffness of the substrate (Allen 1969, Niu and Talreja 1999). On the other hand, the substrate stiffness effectively influences the wrinkling load and wrinkling pattern, such that for stiffer substrates, the wrinkling load is higher and the wrinkling wavelength is slighter (Cerda and Mahadevan 2003). Due to the importance of the substrate stiffness on the wrinkling parameters, great attention must be directed regarding the substrate. Compared with the experimental results and numerical simulations in the literature (Kim *et al*. 2012, Hu *et al*. 2014, Li *et al*. 2011, Lecieux and Bouzidi 2010), deriving the instability parameters of the FG–substrate bounded film analytically through mathematical functions provides more insight into the physics of wrinkling phenomena which is focused in this paper.

In this work, the effect of the substrate nonhomogeinty on the wrinkling parameters is studied. The substrate is assumed as a functionally graded material (FGM) in which its stiffness (i.e. Young's modulus) is non–uniform and changes exponentially along the length span of the film. The uniaxial wrinkling of the film along the length span is considered through the analytical solution of the governing equation of the film–substrate system. It is shown that the non–uniformity of the substrate stiffness has a significant effect on the wrinkling of the film, such that the wrinkling pattern of the film on the FG–substrate is completely different with that of a film–homogeneous substrate. In the latter case, the wrinkles propagate uniformly by a sinusoidal pattern all over the system, while in the former one the wrinkles accumulate around the softest locations of the substrate and a localized wrinkled region develops on the film. Therefore, the effects of the substrate non–uniformity on the wrinkling localization, wrinkling load and wrinkling pattern are investigated.

2. Formulation

Winkler foundation has been widely used to model the interaction of the foundation and the resting beam/plate. By using the Hooke's law of springs, the interaction is modeled as a distributed loading corresponding with the deflection of the beam/film and the stiffness of the foundation. The substrate stiffness of the Winkler model is defined as the elastic modulus (i.e. E) per characteristic depth h of the foundation (Maugis 2013) as $K=E/h$. Therefore, when the elastic modulus E of the foundation is variable, the substrate stiffness K also changes along the domain. This issue can be fostered by using the concept of functionally graded materials (FGM) to introduce a FG–substrate with non–uniform stiffness bounded to the beam/film. According to the literature behind the FG–systems, the gradual change in the composition of the material due to variation of the volume fraction leads to the non–uniform material properties of the system. These non–homogeneity affect on the behavior of the system compared with a homogeneous system with uniform properties all over the domain.

A strip (long slender film) with thickness t, width b and length L deposited on a substrate is shown in Fig. 1. By introducing parameters including $D = Et^3/12(1-v^2)$ as the bending stiffness of the film, $x = \bar{x}/L$ $(0\leq x \leq 1)$ as the dimensionless length variable and $w(x)$ as the normalized deflection of the strip under a uniform in–plane stress resultant along the film span denoted by $\overline{N}_x$ deposited on a Winkler foundation with modulus $\overline{\mathrm{K}}$, the dimensionless governing equation of the thin homogeneous film on the Winkler substrate with uniaxial deformation (strip–like) is represented by Eq. (1) (Reddy 2006)

$$\frac{d^4w}{dx^4} + N\frac{d^2w}{dx^2} + Kw = 0 \tag{1}$$

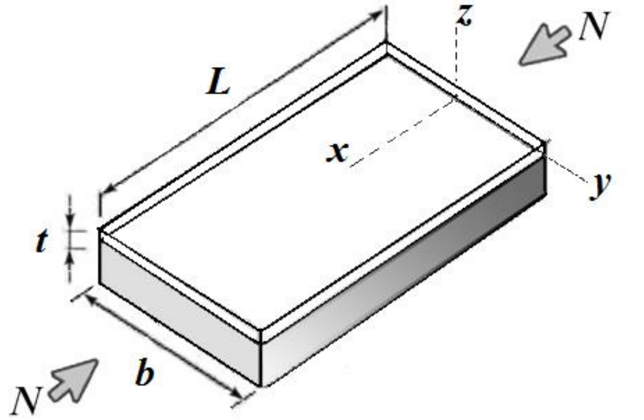

Fig. 1 FG–substrate bounded film under compressive in–plane loading

in which $N=\bar{N}_x L^2/D$ and $K=\bar{K} b L^4/D$ are dimensionless loading and foundation parameters.

In order to make the problem mathematically tractable, the substrate modulus K is assumed as an exponential decaying function as

$$K(x)=K_0\left[1-\varepsilon\ \exp(-\frac{x}{\sigma})\right] \tag{2}$$

where K_0 is the substrate modulus far from the edge x=0, and ε is the amplitude of the stiffness variation with gradient parameter σ. For a homogeneous substrate, the material properties are constant along the entire span corresponding with ε = 0.

Substituting K from Eq. (2) into Eq. (1) leads to a forth order ordinary differential equation with variable coefficients. By using a change of variable as $w(x)=\exp(\alpha x)\,u(x)$ and $x=-\sigma\ \ln(v)$, while α satisfies the relation $\alpha^4+N\alpha^2+K_0=0$, one may show that the ordinary differential equation is represented by Eq. (3) as

$$\begin{aligned}&v^3\frac{d^4u}{dv^4}+(3+a+b+c)v^2\frac{d^3u}{dv^3}\\&+[(1+b+c)a+(1+c)(1+b)]v\frac{d^2u}{dv^2}+c\frac{du}{dv}-u=0\end{aligned} \tag{3}$$

corresponding with the hypergeometric differential equation; while hyper–Bessel functions $_0F_3$ are the general solution of the equation (Kiryakova 1993) as follow

$$_0F_3\left([\ ],[a,b,c];v\right) \tag{4a}$$

$$_0F_3\left([\ ],[2-a,1-a+b,1-a+c];v\right)\ v^{1-a} \tag{4b}$$

$$_0F_3\left([\ ],[2-b,1+a-b,1-b+c];v\right)\ v^{1-b} \tag{4c}$$

$$_0F_3\left([\ ],[2-c,1+b-c,1+a-c];v\right)\ v^{1-c} \tag{4d}$$

and the hypergeometric $_0F_3$ or hyper–Bessel function is defined by a series solution in Eq. (5) as

$$_0F_3\left([\ ],[a,b,c];v\right)=\sum_{m=0}^{\infty}\frac{1}{(a)_m(b)_m(c)_m}\frac{v^m}{m!} \tag{5}$$

where $(a)_m$ is the rising factorial or Pochhammer symbol which is defined by the expression $(a)_m= a\,(a+1)\,(a+2)\ldots(a+m-1)$.

The general solution of the governing equation of the system in Eq. (1) is represented versus four functions $\Phi_k(x)$ (k=1,2,3,4) by Eq. (6) as

$$\begin{aligned}&w(x)=m_1\Phi_1(x)+m_2\Phi_2(x)\\&+m_3\Phi_3(x)+m_4\Phi_4(x)\end{aligned} \tag{6}$$

where

$$\Phi_1(x)=\exp(\beta\eta^+x)\ \phi_1(x) \tag{7a}$$

$$\Phi_2(x)=\exp(\beta\eta^-x)\ \phi_2(x) \tag{7b}$$

$$\Phi_3(x)=\exp(-\beta\eta^+x)\ \phi_3(x) \tag{7c}$$

$$\Phi_4(x)=\exp(-\beta\eta^-x)\ \phi_4(x) \tag{7d}$$

in which

$$\phi_1={}_0F_3\left([],[1-2\theta^+,1-\theta^++\theta^-,1-\theta^+-\theta^-];\mu\right) \tag{8a}$$

$$\phi_2={}_0F_3\left([],[1-2\theta^-,1+\theta^+-\theta^-,1-\theta^+-\theta^-];\mu\right) \tag{8b}$$

$$\phi_3={}_0F_3\left([],[1+2\theta^+,1+\theta^+-\theta^-,1+\theta^++\theta^-];\mu\right) \tag{8c}$$

$$\phi_4={}_0F_3\left([],[1+2\theta^-,1-\theta^++\theta^-,1+\theta^++\theta^-];\mu\right) \tag{8d}$$

and parameters θ and μ in Eq. (8) are represented by $\theta^+=\beta\sigma\eta^+$, $\theta^-=\beta\sigma\eta^-$ and $\mu=\varepsilon\beta^4\sigma^4\exp(-x/\sigma)$ for the sake of simplicity. In addition, other parameters are defined as $\beta=\sqrt[4]{K_0}$, $n=N/\sqrt{4K_0}$, $\eta^+=\sqrt{-n+\sqrt{n^2-1}}$ and $\eta^-=\sqrt{-n-\sqrt{n^2-1}}$.

It is shown that η^+ and η^- are complex conjugate such that $\eta^+\eta^-$=1. Introducing parameters $\eta^+=p+Iq$ and $\eta^-=p-Iq$, where $I=\sqrt{-1}$ is the unit imaginary number, leads to represent $p=\sqrt{(1-n)/2}$ and $q=\sqrt{(1+n)/2}$. On the other hand, from the definition of the hyper–Bessel function in Eq. (5), it is straight forward to show that the functions in Eq. (8) are complex conjugate as presented in Eq. (9)

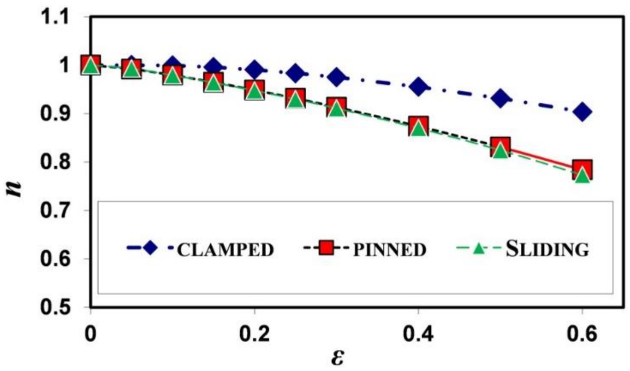

Fig. 2 Dimensionless wrinkling load versus ε for K_0=10^9 and σ=0.05 for a semi–infinite film with different boundary conditions

$$\phi_1(x) = \phi_1^R(x) + I\phi_1^I(x) \tag{9a}$$

$$\phi_2(x) = \phi_1^R(x) - I\phi_1^I(x) \tag{9b}$$

$$\phi_3(x) = \phi_3^R(x) + I\phi_3^I(x) \tag{9c}$$

$$\phi_4(x) = \phi_3^R(x) - I\phi_3^I(x) \tag{9d}$$

Imposing Eq. (9) into (7) with some mathematical treatments leads to the solution of the differential equation (1) in the new format of real parameters $\Psi_k(x)$ (k=1,2,3,4) as

$$w(x) = \exp(\beta px)\left[c_1\Psi_1(x) + c_2\Psi_2(x)\right] + \exp(-\beta px)\left[c_3\Psi_3(x) + c_4\Psi_4(x)\right] \tag{10}$$

where

$$\Psi_1(x) = \phi_1^R(x)\cos(\beta qx) - \phi_1^I(x)\sin(\beta qx) \tag{11a}$$

$$\Psi_2(x) = \phi_1^R(x)\sin(\beta qx) + \phi_1^I(x)\cos(\beta qx) \tag{11b}$$

$$\Psi_3(x) = \phi_3^R(x)\cos(\beta qx) - \phi_3^I(x)\sin(\beta qx) \tag{11c}$$

$$\Psi_4(x) = \phi_3^R(x)\sin(\beta qx) + \phi_3^I(x)\cos(\beta qx) \tag{11d}$$

and c_k's (k=1,2,3,4) are constant parameters determined by imposing the boundary conditions of the film. Among different classical boundary conditions including pinned, sliding, free and clamped conditions, in this work, the clamped boundary conditions of the film at its edges is studied as w= 0 and $dw/dx = 0$ for x_0=0 and 1. Imposing the boundary conditions leads to an algebraic system of equations as $[\Psi_{ij}]\{c_i\} = 0$ (i,j=1,2,3,4). The eigenvalues and eigenfunctions are corresponding with the instability loads and mode shapes of the wrinkling.

On the other hand, for a homogeneous substrate with uniform stiffness $K(x) = K_0$ along the length span (i.e. ε=0), it is shown that the solution of the governing equation is derived versus trigonometric functions as represented in the literature. In the next section, the results of the wrinkling of the FG–substrate are compared with the results of the homogeneous substrate for semi–infinite, infinite and finite length systems.

3. Numerical results and discussion

3.1 Infinite and semi–infinite films

According to the literature of wrinkling of thin films, for a uniform film on a homogeneous substrate with infinite length, a sinusoidal pattern develops along the length span with wavenumber β_0^W under the wrinkling load N_0^W as

$$\beta_0^W = \sqrt[4]{K_0} \tag{12a}$$

$$N_0^W = 2\sqrt{K_0} \tag{12b}$$

corresponding with dimensionless wrinkling load $n = N/N_0^W$ =1 (Birman and Bert 2004, Cerda and Mahadevan 2003, Pocivavsek *et al*. 2008).

On the other hand, for a FG–substrate bounded film with semi–infinite length (i.e. $x \geq 0$), the coefficients c_1 and c_2 in Eq. (10) are zero for a mathematical bounded finite solution. Imposing the boundary conditions at x=0 results in different types of symmetric and antisymmentric modes. By solving the characteristic equation numerically, the wrinkling loads and wrinkling pattern are determined. The boundary conditions at x=0 for clamped edge are given by $w=dw/dx=0$, for hinged edge are imposed as $w=d^2w/dx^2=0$, and for sliding edge are $dw/dx=d^3w/dx^3=0$.

The dimensionless wrinkling load (i.e. $n = N/N_0^W$) versus parameter ε for a sample case of σ=0.05 and K_0 = 10^9 is shown in Fig. 2 for different boundary conditions. The curves start from n=1 corresponding to the homogeneous substrate (i.e. ε = 0) as expected. A regression analysis shows that the curves follow a quadratic relation versus parameter ε as,

$$n = 1 - H(\sigma, K_0)\ \varepsilon^2 \tag{13}$$

Also the wrinkling pattern of the film is shown in Fig. 3 for different boundary conditions and structural parameters (i.e. σ=0.05 and K_0= 10^9 and ε = 0.1, 0.4). According to the results, the semi–infinite film with clamped edge undergoes bigger number of wrinkles, as its wrinkling load is higher than other boundary conditions (i.e. pinned and sliding). So, one may conclude that for a semi-infinite film, the mode corresponding with the clamped edge is not appeared on the film.

On the other hand, for the infinite film deposited on the FG–substrate, the symmetric and anti–symmetric solutions are corresponding with the sliding and hinged boundary conditions as shown in Fig. 3. For both the symmetric and anti–symmetric modes, the wrinkling loads and the patterns are almost same as each other.

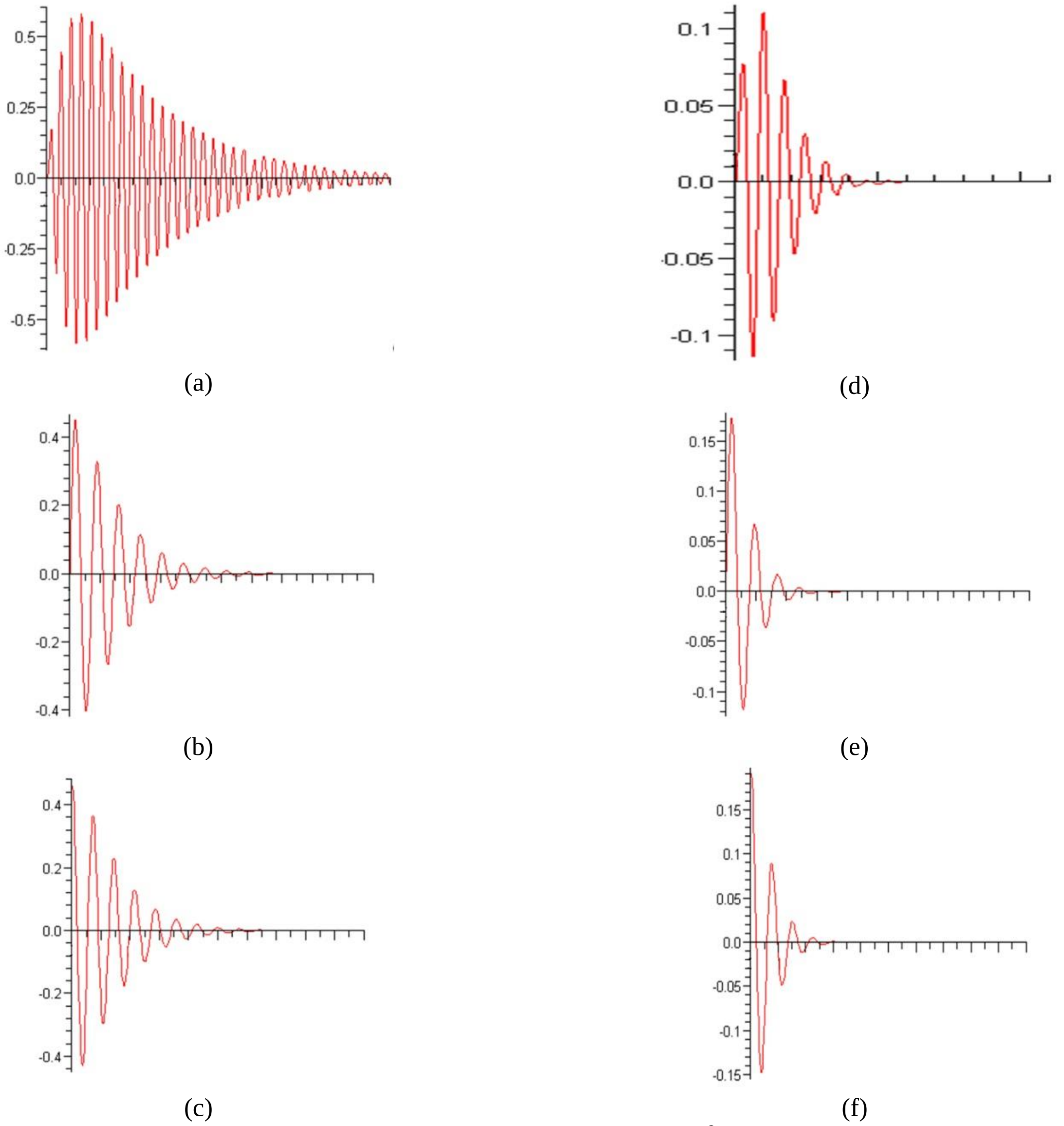

Fig. 3 Wrinkling pattern of a semi–infinite film–substrate for σ = 0.05, K_0=10^9, ε = 0.1 (a,b,c) and ε = 0.4 (d,e,f), with clamped (a,d), pinned (b,e) and sliding (c,f) edge

3.2 Film–substrate with finite length

For a film with finite length deposited on a homogeneous substrate with clamped–clamped boundary conditions, Ratzersdorfer (1936) showed that when the substrate is soft enough, the wavelength of the flexures on the film–substrate is not tiny and the critical compressive load of the instability is represented as the summation of the Euler buckling load of the film and the substrate effect. Obviously, when the thickness of the film is too small and the substrate is not too flabby, the substrate effect is several orders of magnitude larger than the Euler buckling load so that the wrinkling is the dominant phenomenon on the film. Therefore, the wrinkling load N_0^{W} and wavenumber β_0^{W} are represented in terms of the dimensionless substrate stiffness K with Eq. (12) corresponding with dimensionless wrinkling load n=1.

For a film on FG–substrate with non–uniform stiffness, the eigenvalue problem of the system for clamped– clamped boundary conditions is solved for different values of parameters K_0, σ and ε. The first critical wrinkling load versus parameter ε is shown in Fig. 4 for different values of σ=0.05, 0.1, 0.15 and K_0 = 10^8, 10^9, 10^{10}. The graphs follow the descending quadratic relation in Eq. (13) with a high accuracy R^2=0.95. On the other hand, Figs. 5 and 6 show the variation of the parameter n versus σ and K_0. All the curves are descending functions such that by increasing the independent variables (ε, σ and K_0), the dimensionless wrinkling load n decreases.

Finally, a finite difference code is developed to verify the results of the analytical solution using MATLAB software. The wrinkling loads from the finite difference method is completely in match with the results of the analytical solution as plotted in Fig. 7 for a sample case.

Furthermore, The wrinkling pattern is considered for the clamped–clamped film on the FG–substrate and the effect of the parameter ε is clarified (Fig. 8). The figures show that

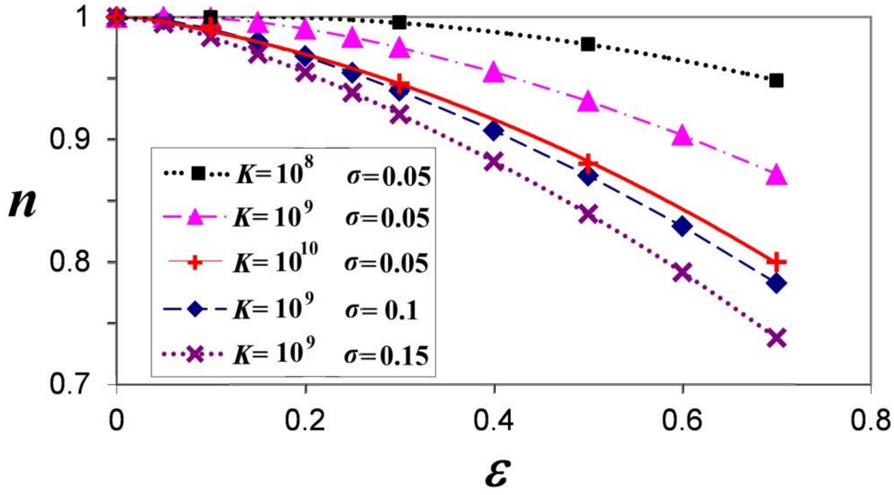

Fig. 4 Critical wrinkling load versus parameter ε for K_0={10^8,10^9, 10^{10}}and σ={0.05, 0.1, 0.15}

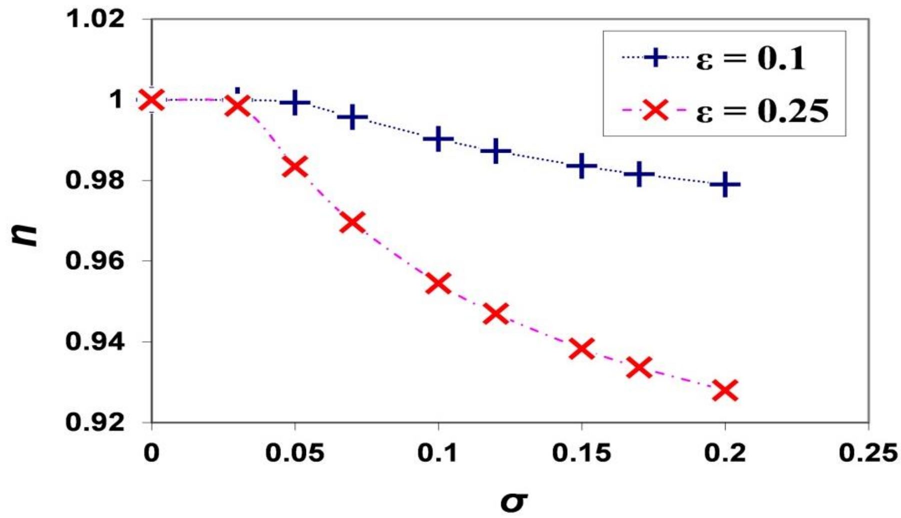

Fig. 5 Dimensionless wrinkling load n versus σ for K_0=10^9

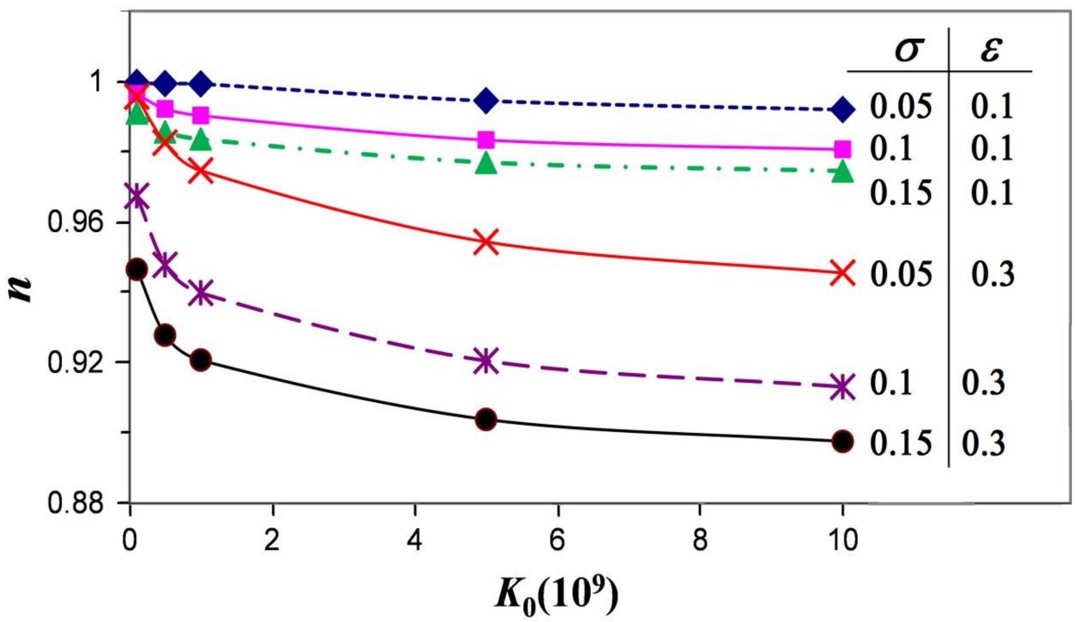

Fig. 6 Dimensionless wrinkling load n versus K_0

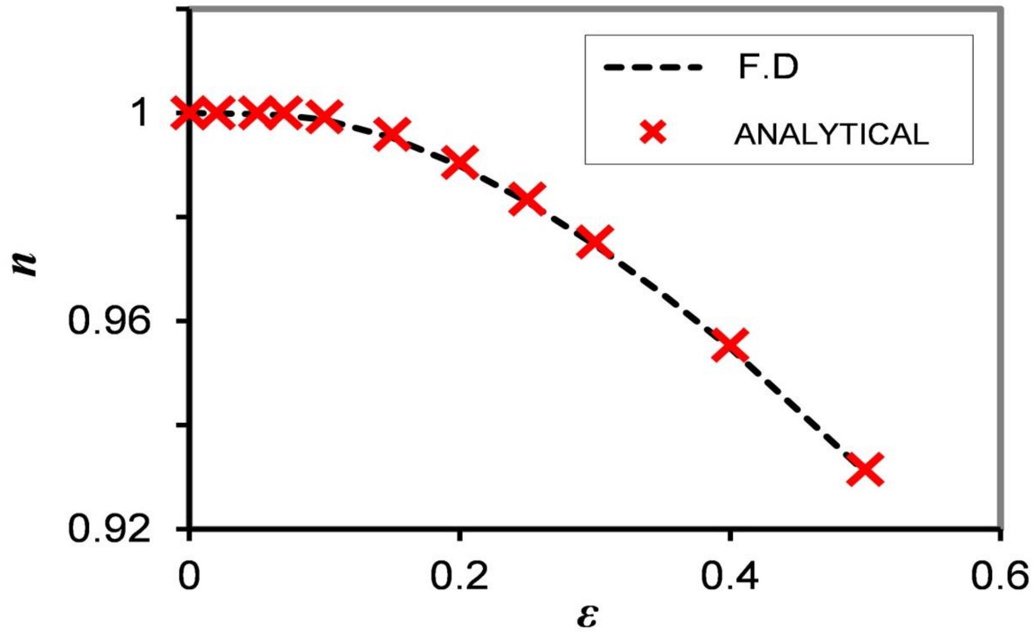

Fig. 7 Normalized wrinkling load versus ε from Finite Difference method (F.D) compared with the analytical solution for σ =0.05 and K_0=10^9

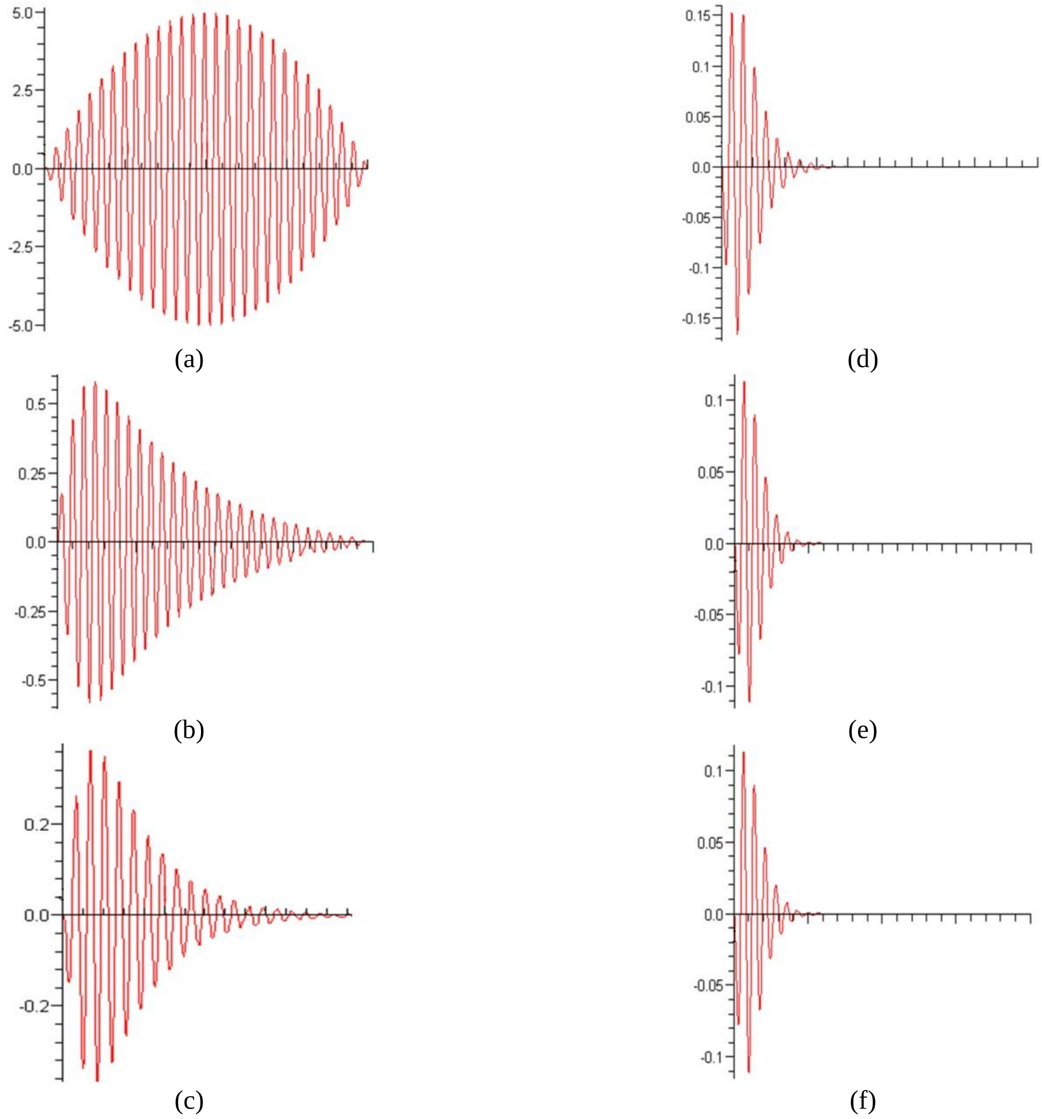

Fig. 8 Wrinkling pattern of a film with clamped edges for σ =0.05 and K_0=10^9

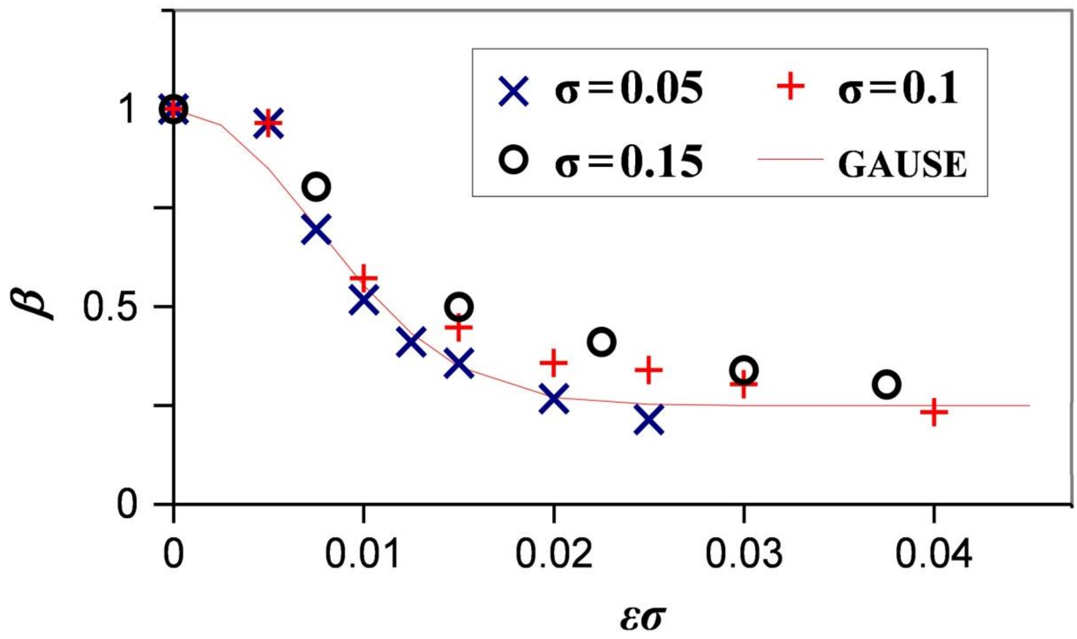

Fig. 9 Normalized apparent wavenumber for K_0=10^9

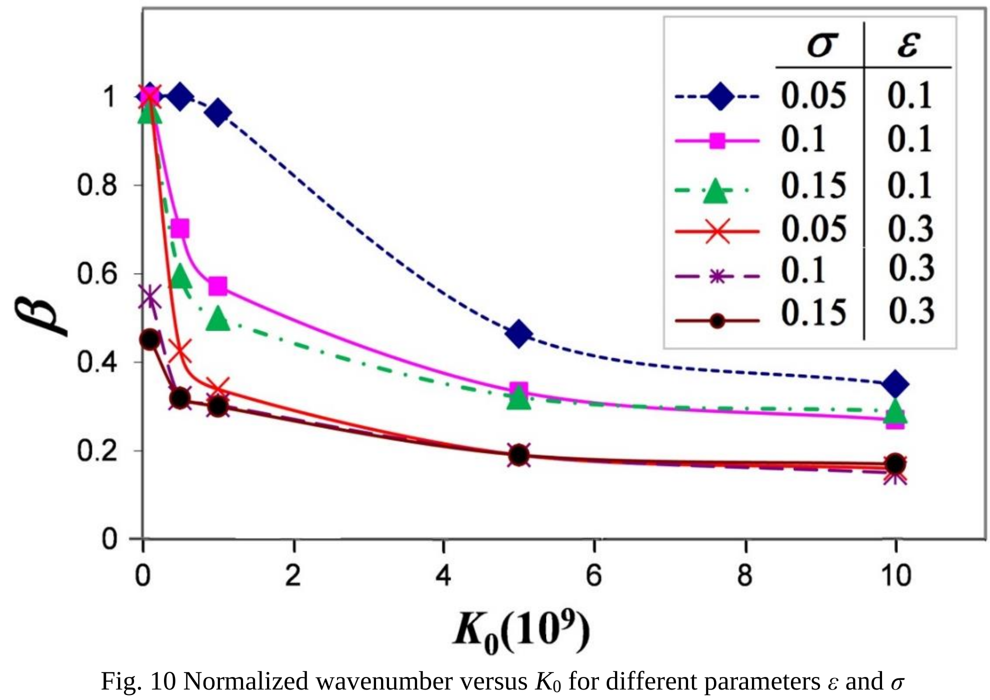

Fig. 10 Normalized wavenumber versus K_0 for different parameters ε and σ

for a homogeneous substrate with ε=0, the pattern is uniform along the span; while increasing the nonhomogeneity of the substrate (i.e. increasing ε) disturbs the uniformity of the wrinkles (Zhao *et al*. 2017). The wavenumber of the wrinkles are discussed as well. According to Eqs. (10) and (11), the wrinkles are periodic. However, the decaying behavior of the wrinkles along the length span leads to define an apparent wavenumber, the number of the wrinkles which appear on the film. The apparent wavenumber is normalized versus the wavenumber in Eq. (12), and is shown with a descending curve like a Gaussian function versus parameters K_0, σ and ε as illustrated in Figs. 9 and 10.

In order to characterize the wrinkling pattern on the film, besides the apparent wavenumber of the wrinkles, another parameter is introduced as footprint of the wrinkles on the film, which represents the apparent length of the film influenced by the wrinkles. As illustrated in Fig. 8, the number of the wrinkles and the footprint of the wrinkling decrease by growing the parameter ε. In other word, smaller section of the film is affected by the wrinkles when the gradient of the FGM substrate increases. A regression

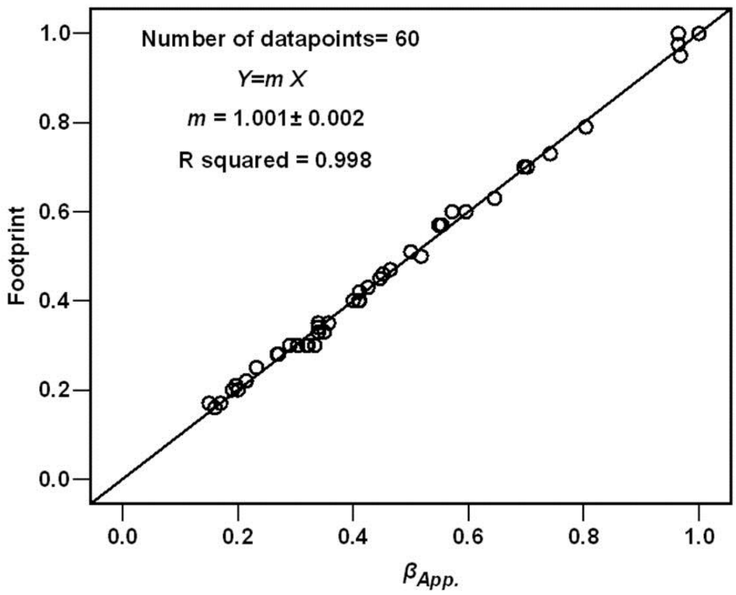

Fig. 11 Footprint of the wrinkling versus wavenumber β for different values of K_0, ε and σ

analysis shows that the footprint of the wrinkling is directly proportional with the apparent wavenumber as shown in Fig. 11 with a high accuracy (R^2=0.998) for 60 datapoints as sample cases.

According to the current analysis, in a FG–substrate bounded film, the gradient of the substrate stiffness has significant effect on the wrinkling pattern such that the wrinkles accumulate densely at the softest location of the substrate with bigger amplitudes similar to Zhao *et al.* (2017). Therefore, the wrinkling pattern is completely different from the uniform wrinkling pattern of a homogeneous substrate–film system reported in the literature. This accumulative effect of the wrinkling opens new windows in physics of wrinkling in thin film structures.

4. Conclusions

The uniaxial wrinkling problem of a homogeneous thin film deposited on a FGM substrate is studied and the wrinkling parameters (i.e. load and pattern) are determined analytically. The FGM substrate is modeled by using a Winkler foundation in which the stiffness of the foundation is non–uniform along the span with a variable stiffness. For an exponential stiffness profile of the FGM substrate, the governing equation is solved analytically in terms of hyper–Bessel functions. The problem is investigated for infinite, semi–infinite and finite length of the film–substrate system. In contrast with a homogeneous substrate–bounded film with uniform stiffness in which the wrinkles propagate along the length span uniformly, the results of this work show that the non–uniformity of the FGM substrate disturbs the wrinkling pattern so that the wrinkles accumulate around the location of the substrate with less stiffness and the amplitude of the wrinkles in this region grows. Increasing the gradient of the FGM substrate intensifies this accumulative effect by decreasing the wrinkling load and the effective length of the film influenced by the wrinkles (i.e. Footprint of the wrinkles on the film). Besides the possible applications in thin–film metrology and surface patterning in different fields including experimental works, science and industry; the results of this work may find useful to provide insight into the wrinkling phenomena of various living tissues.

Acknowledgments

The research described in this paper was financially supported by the Islamic Azad University (Karaj Branch) under grant number 152228.

References

Aberle, A.G. (2009), “Thin–film solar cells”, *Thin Solid Films*, **517**(17), 4706-4710. https://doi.org/10.1016/j.tsf.2009.03.056.

Allen, H.G. (1969), *Analysis and Design of Structural Sandwich Panels*, Pergamon Press, Oxford, UK.

Amar, M.B. and Bordner, A. (2017), “Mimicking cortex convolutions through the wrinkling of growing soft bilayers”, *J. Elasticity*, **129**(1-2), 213-238. https://doi.org/10.1007/s10659-017-9622-9.

Birman, V. and Bert, C.W. (2004), “Wrinkling of composite–facing sandwich panels under biaxial loading”, *J. Sandw. Struct. Mater.*, **6**(3), 217-237. https://doi.org/10.1177/1099636204033643.

Cao, Y.P., Jia, F., Zhao, Y., Feng, X.Q. and Yu, S.W. (2012), “Buckling and post–buckling of a stiff film resting on an elastic graded substrate”, *Int. J. Solids Struct.,* **49**(13), 1656-1664. https://doi.org/10.1016/j.ijsolstr.2012.03.004.

Cerda, E., Ravi-Chandar, K. and Mahadevan, L. (2002), “Thin films: Wrinkling of an elastic sheet under tension”, *Nature*, **419**(6907), 579. https://doi.org/10.1038/419579b.

Cerda, E. and Mahadevan, L. (2003), “Geometry and physics of wrinkling”, *Phys. Rev. Lett.*, **90**(7), 074302. https://doi.org/10.1103/PhysRevLett.90.074302.

Cerda, E. (2005), “Mechanics of scars”, *J. Biomech.*, **38**(8), 1598-

1603. https://doi.org/10.1016/j.jbiomech.2004.07.026.
Chen, X. and Hutchinson, J.W. (2004), "Herringbone buckling patterns of compressed thin films on compliant substrates", *J. Appl. Mech.*, **71**(5), 597-603. https://doi.org/10.1115/1.1756141.
Chen, L., Zhang, Y., Swaddiwudhipong, S. and Liu, Z. (2014), "Mimicking the pattern formation of fruits and leaves using gel materials", *Struct. Eng. Mech.*, **50**(5), 575-588. https://doi.org/10.12989/sem.2014.50.5.575.
Chen, Z., Chen, W. and Song, J. (2017), "Buckling of a stiff thin film on an elastic graded compliant substrate", *Proc. Royal Soc. A*, **473**(2208), 20170410. https://doi.org/10.1098/rspa.2017.0410.
Clark, B.R., Pantoya, M.L., Hunt, E.M., Kelly, T.J., Allen, B.F., Heaps, R.J. and Daniels, M.A. (2015), "Synthesis and characterization of flexible, free–standing, energetic thin films", *Surf. Coat. Tech.*, **284**, 422-426. https://doi.org/10.1016/j.surfcoat.2015.05.048.
Fu, C., Xu, F. and Huo, Y. (2018), "Photo–controlled patterned wrinkling of liquid crystalline polymer films on compliant substrates", *Int. J. Solids Struct.*, **132**, 264-277. https://doi.org/10.1016/j.ijsolstr.2017.10.018.
Genzer, J. and Groenewold, J. (2006), "Soft matter with hard skin: From skin wrinkles to templating and material characterization", *Soft Matter*, **2**(4), 310-323. https://doi.org/10.1039/B516741H.
Howarter, J.A. and Stafford, C.M. (2010), "Instabilities as a measurement tool for soft materials", *Soft Matter*, **6**(22), 5661-5666. https://doi.org/10.1039/C0SM00365D.
Hu, J., He, Y., Lei, J., Liu, Z. and Swaddiwudhipong, S. (2014), "Mechanical behavior of composite gel periodic structures with the pattern transformation", *Struct. Eng. Mech.*, **50**(5), 605-616. https://doi.org/10.12989/sem.2014.50.5.605.
Jia, Z. and Li, T. (2016), "Failure mechanics of a wrinkling thin film anode on a substrate under cyclic charging and discharging", *Extreme Mechanics Letters*, **8**, 273-282. https://doi.org/10.1016/j.eml.2016.03.006.
Karki, S., Kim, H., Na, S.J., Shin, D., Jo, K. and Lee, J. (2016), "Thin films as an emerging platform for drug delivery", *Asian Journal of Pharmaceutical Sciences*, **11**(5), 559-574. https://doi.org/10.1016/j.ajps.2016.05.004.
Kim, T.Y., Puntel, E. and Fried, E. (2012), "Numerical study of the wrinkling of a stretched thin sheet", *Int. J. Solids Struct.*, **49**(5), 771-782. https://doi.org/10.1016/j.ijsolstr.2011.11.018.
Kiryakova, V.S. (1993), *Generalized Fractional Calculus and Applications*, CRC press.
Kudrolli, A. and Chopin, J. (2018), "Tension–dependent transverse buckles and wrinkles in twisted elastic sheets", *Proc. Royal Soc. A*, **474**(2214), 20180062. https://doi.org/10.1098/rspa.2018.0062.
Lecieux, Y. and Bouzidi, R. (2010), "Experimental analysis on membrane wrinkling under biaxial load–Comparison with bifurcation analysis", *Int. J. Solids Struct.*, **47**(18-19), 2459-2475. https://doi.org/10.1016/j.ijsolstr.2010.05.005.
Lee, D., Triantafyllidis, N., Barber, J.R. and Thouless, M.D. (2008), "Surface instability of an elastic half space with material properties varying with depth", *J. Mech. Phys. Solids*, **56**(3), 858-868. https://doi.org/10.1016/j.jmps.2007.06.010.
Li, B., Cao, Y.P., Feng, X.Q. and Gao, H. (2011), "Surface wrinkling of mucosa induced by volumetric growth: theory, simulation and experiment", *J. Mech. Phys. Solids*, **59**(4), 758-774. https://doi.org/10.1016/j.jmps.2011.01.010.
Mahendran, M. and Jeevaharan, M. (1999), "Local buckling behaviour of steel plate elements supported by a plastic foam material", *Struct. Eng. Mech.*, **7**(5), 433-445. http://dx.doi.org/10.12989/sem.1999.7.5.433.
Maugis, D. (2013), *Contact, Adhesion and Rupture of Elastic Solids,* (Vol. 130), Springer Science & Business Media, NY, USA.
Niu, K. and Talreja, R. (1999), "Modeling of wrinkling in sandwich panels under compression", *J. Eng. Mech.*, **125**(8), 875-883. https://doi.org/10.1061/(ASCE)0733-9399(1999)125:8(875).
Nolte, A.J., Chung, J.Y., Davis, C.S. and Stafford, C.M. (2017), "Wrinkling–to–delamination transition in thin polymer films on compliant substrates", *Soft Matter*, **13**(43), 7930-7937. http://dx.doi.org/10.1039/C7SM01472D.
Noroozi, M. and Jiang, L. (2012), "Buckling and wrinkling of a functionally graded material (FGM) thin film", *Int. J. Appl. Mech.*, **4**(02), 1250012. https://doi.org/10.1142/S1758825112500123.
Pocivavsek, L., Dellsy, R., Kern, A., Johnson, S., Lin, B., Lee, K. Y.C. and Cerda, E. (2008), "Stress and fold localization in thin elastic membranes", *Science*, **320**(5878), 912-916. https://doi.org/10.1126/science.1154069.
Ratzersdorfer, J. (1936), *Die Knickfestigkeit von Stäben und Stabwerken*, Springer–Verlag.
Reddy, J.N. (2006), *Theory and Analysis of Elastic Plates and Shells*, (2nd Edition), CRC Press, FL, USA.
Song, J. (2010), "Herringbone buckling patterns of anisotropic thin films on elastomeric substrates", *Appl. Phys. Lett.*, **96**(5), 051913. https://doi.org/10.1063/1.3309696.
Veronese, G.P., Allegrezza, M., Canino, M., Centurioni, E., Ortolani, L., Rizzoli, R., Morandi, V. and Summonte, C. (2015), "Graphene as transparent conducting layer for high temperature thin film device applications", *Sol. Energy Mater. Sol. Cells*, **138**, 35-40. https://doi.org/10.1016/j.solmat.2015.02.026.
Vonach, W.K. and Rammerstorfer, F.G. (2001), "A general approach to the wrinkling instability of sandwich plates", *Struct. Eng. Mech.*, **12**(4), 363-376. https://doi.org/10.12989/sem.2001.12.4.363.
Wang, Y.H., Tham, L.G. and Cheung, Y.K. (2005), "Beams and plates on elastic foundations: a review", *Progress in Structural Engineering and Materials*, **7**(4), 174-182. https://doi.org/10.1002/pse.202.
Wang, C.G., Liu, Y.P., Lan, L., Li, L. and Tan, H.F. (2016), "Post–wrinkling analysis of a torsionally sheared annular thin film by using a compound series method", *Int. J. Mech. Sci.*, **110**, 22-33. https://doi.org/10.1016/j.ijmecsci.2016.02.011.
Xu, R., Li, D., Liu, W., Jiang, J., Liao, Y. and Wang, J. (2015a), "Modified nonlinear force density method for form–finding of membrane SAR antenna", *Struct. Eng. Mech.*, **54**(6), 1045-1059. http://dx.doi.org/10.12989/sem.2015.54.6.1045.
Xu, F., Potier-Ferry, M., Belouettar, S. and Hu, H. (2015b), "Multiple bifurcations in wrinkling analysis of thin films on compliant substrates", *Int. J. Nonlin. Mech.*, **76**, 203-222. https://doi.org/10.1016/j.ijnonlinmec.2014.12.006.
Yu, S., Sun, Y., Ni, Y., Zhang, X. and Zhou, H. (2016), "Controlled formation of surface patterns in metal films deposited on elasticity-gradient PDMS substrates", *ACS Appl. Mater. Interfaces*, **8**(8), 5706-5714. https://doi.org/10.1021/acsami.5b12369.
Zhang, Y., Zheng, J., Fang, C., Li, Z., Zhao, X., Li, Y., Ruan, X. and Dai, Y. (2018), "Enhancement of silicon–wafer solar cell efficiency with low–cost wrinkle antireflection coating of polydimethylsiloxane", *Sol. Energy Mater. Sol. Cells*, **181**, 15-20. https://doi.org/10.1016/j.solmat.2017.10.004.
Zhao, J., Guo, X. and Lu, L. (2017), "Controlled wrinkling analysis of thin films on gradient substrates", *Appl. Math. Mech.*, **38**(5), 617-624. https://doi.org/10.1007/s10483-017-2199-9.
Zheng, Y., Li, G.Y., Cao, Y. and Feng, X.Q. (2017), "Wrinkling of a stiff film resting on a fiber–filled soft substrate and its potential application as tunable metamaterials", *Extreme Mechanics Letters*, **11**, 121-127. https://doi.org/10.1016/j.eml.2016.12.002.

PL

Nomenclature

Symbol	Description
b	Width of the system
D	Bending stiffness of the film
E	Young's Modulus
K	Substrate stiffness modulus
h	Substrate depth
L	Length
N,n	Inplane force
t	Thickness
x	length span coordinate
w	Deflection
β	Wavenumber of wrinkles
ε,σ	Substrate gradient parameters
F	Hypergeometric function
$\Gamma\Phi\Psi\theta\varphi\nu pqHu$	Mathematical dummy variables